ROYAL SOCIETY OF CHEMISTRY

PAPER

Check for updates

Effect of non-covalent self-dimerization on the spectroscopic and electrochemical properties of mixed Cu(I) complexes†

Joaquín Cáceres-Vásquez, [a] Danilo H. Jara, [b] Juan Costamagna, [af] Fabián Martínez-Gómez, [af] Carlos P. Silva, [f] Luis Lemus, [f] Eleonora Freire, [cde] Ricardo Baggio, [c] Cristian Vera [*a] and Juan Guerrero [*a]

A series of six new Cu(I) complexes with ([Cu(N-{4-R}pyridine-2-yl-methanimine)(PPh$_3$)Br]) formulation, where R corresponds to a donor or acceptor p-substituent, have been synthesized and were used to study self-association effects on their structural and electrochemical properties. X-ray diffraction results showed that in all complexes the packing is organized from a dimer generated by supramolecular π stacking and hydrogen bonding. ^{1}H-NMR experiments at several concentrations showed that all complexes undergo a fast-self-association monomer–dimer equilibrium in solution, while changes in resonance frequency towards the high or low field in specific protons of the imine ligand allow establishing that dimers have similar structures to those found in the crystal. The thermodynamic parameters for this self-association process were calculated from dimerization constants determined by VT-^{1}H-NMR experiments for several concentrations at different temperatures. The values for K_D (4.0 to 70.0 M^{-1} range), ΔH (−1.4 to −2.6 kcal mol^{-1} range), ΔS (−0.2 to 2.1 cal mol^{-1} K^{-1} range), and ΔG_{298} (−0.8 to −2.0 kcal mol^{-1} range) are of the same order and indicate that the self-dimerization process is enthalpically driven for all complexes. The electrochemical profile of the complexes shows two redox Cu(II)/Cu(I) processes whose relative intensities are sensitive to concentration changes, indicating that both species are in chemical equilibrium, with the monomer and the dimer having different electrochemical characteristics. We associate this behaviour with the structural lability of the Cu(I) centre that allows the monomeric molecules to reorder conformationally to achieve a more adequate assembly in the non-covalent dimer. As expected, structural properties in the solid and in solution, as well as their electrochemical properties, are not correlated with the electronic parameters usually used to evaluate R substituent effects. This confirms that the properties of the Cu(I) complexes are usually more influenced by steric effects than by the inductive effects of substituents of the ligands. In fact, the results obtained showed the importance of non-covalent intermolecular interactions in the structuring of the coordination geometry around the Cu centre and in the coordinative stability to avoid dissociative equilibria.

Introduction

The high versatility of transition metal compounds is a well-known fact, and therefore several studies have been oriented towards an adequate control of their properties through suitable ligand selection. In particular, Cu(I) coordination complexes with bidentate nitrogen donor ligands have been given considerable attention due to their interesting photophysical and

^{a}Laboratorio de Compuestos de Coordinación y Química Supramolecular, Facultad de Química y Biología, Universidad de Santiago de Chile, Av. Libertador Bernardo O'Higgins 3363, Estación Central, Casilla 40, Correo 33, Santiago, Chile. E-mail: juan.guerrero@usach.cl; cristian.veraoy@usach.cl

^{b}Facultad de Ingenieria y Ciencias, Universidad Adolfo Ibáñez, Av. Padre Hurtado 750, Viña del Mar, Chile

^{c}Gerencia de Investigación y Aplicaciones, Centro Atómico Constituyentes, Comisión Nacional de Energía Atómica, Avenida Gral. Paz 1499, 1650, San Martín, Buenos Aires, Argentina. E-mail: baggio@tandar.cnea.gov.ar

^{d}Escuela de Ciencia y Tecnología, Universidad Nacional de San Martín, Argentina and Gerencia de Investigación y Aplicaciones, Centro Atómico Constituyentes, Comisión Nacional de Energía Atómica, Buenos Aires, Argentina

^{e}Member of CONICET, Argentina

^{f}Facultad de Química y Biología, Universidad de Santiago de Chile, Av. Libertador Bernardo O'Higgins 3363, Estación Central, Casilla 40, Correo 33, Santiago, Chile

† Electronic supplementary information (ESI) available. X-ray crystallographic files in cif format for the structures of the complexes of [Cu(NN′-R) (PPh$_3$)Br] (R = NO$_2$, COCH$_3$, H, CH$_3$, OCH$_3$, N(CH$_3$)$_2$) have been deposited. CCDC 1559217–155922. For ESI and crystallographic data in CIF or other electronic format see DOI: https://doi.org/10.1039/d2ra05341a

electrochemical behaviour with potential applications in solar energy conversion, luminescence-based sensing, display devices, molecular switches, probes of biological systems, and catalysis.[1] Also, these complexes have played an important role in the construction of sophisticated molecular architectures and contributed to the development and great growth of supramolecular chemistry[2] and material science.[3]

Cu(I) is a structurally labile metal centre which can experience ligand exchange and also distortions of its ideal tetrahedral geometry, where both coordinative and conformational labilities of the Cu(I) complexes are ascribed to the lack of crystal field stabilization due to its d^{10} full shell configuration.[4] Such dynamic behaviour has a direct impact on the redox stability of cuprous complexes or the establishment of equilibria in solution.[4,5]

The inclusion of bulky substituents adjacent to the coordinating nitrogen atoms in homoleptic $[Cu(NN)_2]^+$ and heteroleptic $[Cu(NN)(PPh_3)_2]^+$ complexes, with NN = symmetrical chelating diimines ligands, for example neocuproine (Fig. 1a), has been the first reported strategy to improve its photophysical performance by way of restricting the tetrahedral to the square-planar flattening, in accordance with the structural requirements of the metal, formally Cu^{2+} in the excited state. The possibility of Cu(I) complexes to reach a more flattened conformation is also responsible for their oxidation to cupric species in solution.[4d,6]

Also, the influence of intramolecular non-covalent interactions on both chemical stabilization and electronic and emissive properties of Cu(I) complexes has been established, indicating that properties of Cu(I) complexes are not uniquely determined by structural effects of the ligand and that non-covalent interactions can play an important role on their behaviour.[7]

The presence of intermolecular π stacking aggregations in transition metal complexes with aromatic ligands has been well established in the solid state.[8] However, the evidence of discrete dimers in solution is limited to a few examples.[9] These structures have been identified by ^{1}H-NMR in square-planar and octahedral metallic complexes where the supramolecular systems are supported by face–face (π–π) and face–edge (H···π) interactions between ligands possessing extensive aromatic systems.
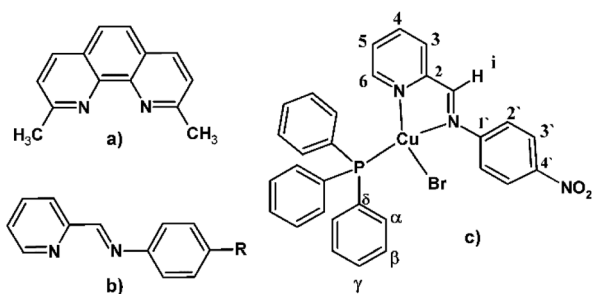
On the other hand, bi-coordinating pyridine-imine type Schiff bases (Fig. 1b) are more flexible than polypyridines and rigid polyaromatic ligands and can be useful tools for the design of conformationally labile Cu(I) complexes that allow the establishment of intermolecular interactions. However, studies of pyridine-imine Cu(I) complexes as supramolecular materials as very limited, and most of the structural information on these systems has been obtained from studies regarding their catalytic,[1p,q,10] and emissive properties.[1a,10a,11]

One of the few examples of supramolecular dimers of Cu(I) complexes with experimental evidence of self-association both in solution and in the solid phase by NMR spectroscopy and X-ray diffraction, respectively, has been reported for the mixed complex [Cu(N-{4-nitrophenyl}pyridine-2-yl-methanimine)(PPh_3)Br],[12] in which the imine ligand possess a small aromatic system (Fig. 2).

For this complex, the monometallic structure corresponds to a slightly distorted tetrahedral complex. However, two non covalent forces, π-stacking and C–H···Br interactions are jointly acting to produce a discrete dimer. The NMR results showed the presence of an equilibrium between both monometallic and supramolecular bimetallic complexes. This dynamic behaviour in solution was interpreted as a self-dimerization process enthalpically driven through the formation of both π–π and C–H···Br interactions previously indicated where such a supramolecule retains a structure similar to that observed in the packing of its crystal structure.[12]

As a continuation of this work and with the aim of understanding more about this self-dimerization in neutral mixed Cu(I) complexes, a series of similar Cu(I) complexes, [Cu(NN'-R)(PPh_3)Br], (PPh_3 = triphenylphosphine, NN'-R = N-p-R-phenyl-pyridine-2-yl-me-thanimine, R = NO_2, COCH_3, Cl, H, CH_3, OCH_3 and N(CH_3)_2) were synthesized and characterized (Fig. 1c). These ligands include a series of substituents with different electronic characteristics in the *para* position so as not to cause a great conformational impact. The molecular structures and the presence of supramolecular dimers in the solid are discussed by interpretation of X-ray crystallographic data, while the evaluation of the structure
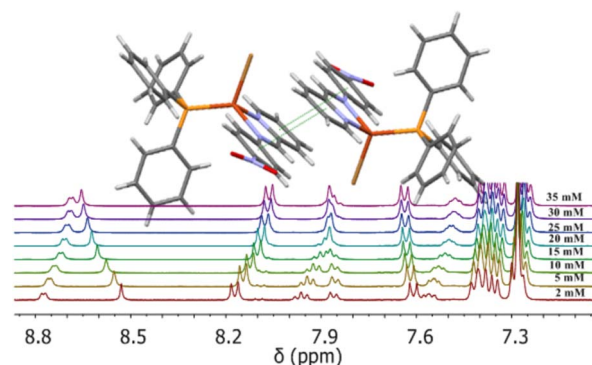

Fig. 1 (a) Neocuproine. (b) Pyridine-imine type ligand. (c) General chemical structure of the [Cu(NN'-R)(PPh_3)Br] complexes, including the labelling scheme used in the NMR assignments.

Fig. 2 ^{1}H-NMR spectra of [Cu(N-{4-nitrophenyl}pyridine-2-yl-methan-imine)(PPh_3)Br]_2 complex as a function of concentration. (Insert) Scheme showing the dimer formed in the crystalline packing by both π–π and C–H···Br interactions around an inversion centre.

and the presence of dimers in solution are studied by ^{1}H-NMR. The dynamic behaviour of these systems was studied by ^{1}H-NMR-VT for several concentrations and temperatures. The impact of this supramolecular behaviour on the electronic properties of this set of complexes is evaluated through electrochemical studies.

Results and discussion

Synthesis and characterization

The [Cu(NN'-R)(PPh$_3$)Br] complexes were synthesized by the template condensation method from equimolar amounts of reagents as shown schematically in Scheme 1.[2e,g]

The structures of the complexes were unequivocally established by the concerted use of several NMR techniques from chloroform-d solutions, i.e. 1D NMR (^{1}H-NMR, {^{1}H}^{13}C-NMR, {^{1}H} ^{31}P-NMR), and 2D NMR (COSY, HSQC, HMBC). The general and specific synthetic procedure and the NMR characterization data are reported in the Experimental section and ESI.†

Crystals of the complexes suitable for X-ray crystallographic analysis were obtained by slow ether diffusion into a dichloromethane solution of the complexes, and their crystal structures were solved for [Cu(NN'-R)(PPh$_3$)Br] with R = COCH$_3$, H, CH$_3$, OCH$_3$, and N(CH$_3$)$_2$. The crystal structure could not be obtained for the Cu(NN'-Cl)(PPh$_3$)Br] complex, but its structure was determined by NMR techniques since all the complexes showed chemical stability in the time periods used for both NMR and electrochemical studies. All dynamic studies by ^{1}H-NMR from chloroform solutions, and the electrochemical measurements were carried out from crystalline samples of the complexes. The
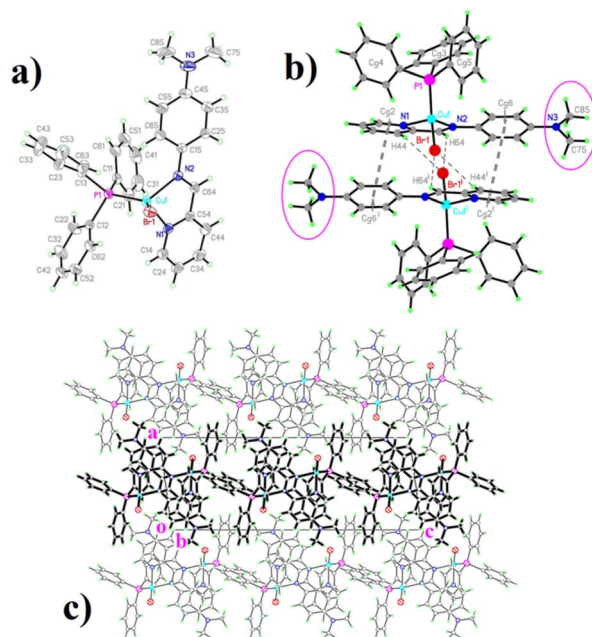

Fig. 3 Molecular (a), dimers (b), and packing (c) diagrams for [Cu(NN'-N(CH$_3$)$_2$)(PPh$_3$)Br] (a) displacement ellipsoids are drawn at a 30% level. (b) Bold dashed lines represent π−π bonds; simple dashed lines represent C−H···Br bonds. Circled is the N(CH$_3$)$_2$ substituent. (c) Viewed in projection, the (100) slabs generated by interaction #4 (One of these slabs has been highlighted for clarity). Non covalent interactions are omitted.

accurate proton assignments for each temperature and concentration were confirmed by COSY experiments; in the same way, NOESY experiments for evaluating the structure of supramolecular adducts at some of the temperatures and concentrations used were carried out. The [Cu(N-p-NO$_2$-phenyl-pyridine-2-yl-methanimine)(PPh$_3$)Br] complex has been previously published, and the reported data were used for comparative analyses.[12]

Crystallographic structures

The structural drawings of the [Cu(N-p-dimethylamine-phenyl-pyridine-2-yl-methanimine)(PPh$_3$)Br] complex are shown in
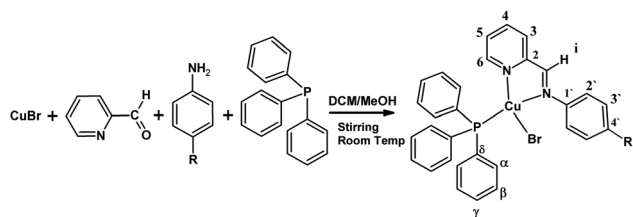
Scheme 1

Table 1 Selected coordination parameters, (distances/Å and angles/°) for [Cu(NN'-R)(PPh$_3$)Br] complexes

−R	(−NO$_2$)	(−COCH$_3$)	(−H)	(−CH$_3$)	(−OCH$_3$)	(−N(CH$_3$)$_2$)
Distances						
Cu1−N1	2.096(3)	2.115(5)	2.1222(18)	2.094(3)	2.102(3)	2.1015(17)
Cu1−N2	2.109(3)	2.095(5)	2.1169(18)	2.101(3)	2.097(2)	2.1015(17)
Cu1−P1	2.1946(10)	2.1833(16)	2.1991(6)	2.1848(9)	2.1994(9)	2.1906(6)
Cu1−Br1	2.421(6)	2.4237(10)	2.4376(4)	2.4233(5)	2.4499(5)	2.3811(4)
Angles						
N1−Cu1−N2	79.10(12)	78.8(2)	79.00(7)	79.09(12)	79.23(12)	79.67(7)
N1−Cu1−P1	117.07(9)	118.93(16)	124.52(5)	117.08(8)	118.05(7)	104.60(5)
N1−Cu1−Br1	106.34(8)	105.63(16)	102.94(5)	106.16(7)	112.15(7)	113.56(5)
N2−Cu1−P1	124.56(9)	127.36(16)	119.59(5)	122.42(7)	125.12(7)	112.02(5)
N2−Cu1−Br1	108.12(8)	105.37(15)	107.40(5)	108.50(7)	104.94(7)	112.38(5)
P1−Cu1−Br1	115.45 (3)	114.50(5)	116.77(2)	116.97(3)	112.93(3)	125.155(19)

Fig. 3 (a): displacement ellipsoid representation; (b): dimeric structure, and (c): packing organization. The same representations for the five other [Cu(NN'-R)(PPh₃)Br] complexes are available as ESI (Fig. SI1a–c to SI5a–c†). Crystal and data collection parameters are available in Table SI1.† Selected coordination parameters are given in Table 1, while non-covalent interactions are given in Tables SI2 (π–π) and SI3† (C–H···X, X = Br, O, π). In these latter tables a #n code has been included to facilitate interaction identification and consequently, the packing description.

From a molecular point of view, the structures are quite similar (Fig. 3a and SI1a to SI5a†), with a tetracoordinate Cu(I) ion bonded to the corresponding pyridine-imine chelating ligand and the remaining coordination sites being completed by a PPh₃ group and a bromine anion. Coordination bond distances and angles (Table 1) do not depart significantly from reported values in similar systems.[10,11,14]

In all complexes, the geometry around copper is that of a distorted tetrahedron, elongated along the common bisector of the small N–Cu–N angle and the larger P–Cu–Br one. The N–Cu–N angle is very similar to the one observed in complexes with polypyridine and pyridine-imine ligands (around 80°). As a reference, the bite angles of pyridine-imine ligands similar to those used in this work, in rhenium, rhodium, and iridium complexes are N–Re–N: 74.82,[15] N–Rh–N: 79.38,[16] N–Ir–N: 76.84.[17]

While the N–Cu–N angle remains relatively constant, the remaining coordination angles in the polyhedra show some differences through the series, but no correlation with the electronic effect of the substituent is observed.

The rather weak inter-molecular contacts are also similar in almost all complexes, and the most remarkable are the stacking contacts built around inversion centres of the phenyl/py fragments in the structures of all complexes with the exception of the py/py stacking exhibited by the [Cu(NN'-H)(PPh₃)Br] complex (Table 2), which in all cases lead to the formation of some kind of weakly linked dimeric units (Fig. 3b and SI1b to SI4b, Table SI2†).

Even if these π–π interactions between extended aromatic systems (shown in double dashed lines) are the main ones responsible for the dimeric organization, there are some further weak C–H···Br contacts (drawn in simple dashed lines) that reinforce this inter-molecular linkage. The way in which this is achieved is quite similar in five of these six structures, either through the C44–H44···Br1 or the C64–H64···Br1 contacts, or eventually through both.

Contrasting with these five structures, the dimer in the [Cu(NN'-H)(PPh₃)Br] structure appears different, held together by a strong face–face py/py (π–π) and two extensive face-edge (CH···π) interactions[18] (Fig. SI5b,† Table 2). Furthermore, this structure is the only one with a significant intra-molecular C–H···Br interaction.

The C–H···X$_{neighbour}$ interactions left (X = Br, O, π), characterized in Table SI3† by the remaining sym-codes (i), are inter-dimeric in nature, and result in the formation of a diversity of packing motifs shown in Fig. 4c and SI1c to SI5c of the ESI.†

Regarding the way in which this is achieved, there are some common features grouping structures together. Thus, structures for complexes with R = NO₂, COCH₃ and CH₃, are nearly isostructural, and this shows up in the packing, where the C34–H34···Br1' interactions (#4 in [Cu(NN'-NO₂)(PPh₃)Br] and [Cu(NN'-COCH₃)(PPh₃)Br], #3 in [Cu(NN'-CH₃)(PPh₃)Br]), give rise to columns directed along b, while the remaining ones link these 1D substructures transversally (along c) to form one-dimer-thick 2D arrays parallel to (100) (Fig. SI1c to SI3c†).

On the other hand, structures [Cu(NN'-OCH₃)(PPh₃)Br] and [Cu(NN'-H)(PPh₃)Br] follow a similar pattern, in spite of the differences in the dimer's shape: there is a leading interaction (#3 and #5 in Table SI3†) defining columns along b, and the remaining ones linking them along c in [Cu(NN'-H)(PPh₃)Br] and along a in [Cu(NN'-OCH₃)(PPh₃)Br], to define planar arrays parallel to (100) and (001), respectively (Fig. SI4c and SI5c†).

Finally, the structure of [Cu(NN'-N(CH₃)₂)(PPh₃)Br] is slightly different, with interaction #4 (Table SI3†) defining "*per se*" a 2D array parallel to (100), the remaining ones interlinking these slabs into a complex 3D structure (Fig. 3c).

The eventual effect of the *para*-substituents on the phenyl ring over the dimeric structures was analyzed by comparison in the series of some relevant molecular parameters (*e.g.*), the interligand dihedral angles between phenyl and pyridine aromatic rings, the NCCN ligand torsion angles in the coordination environment, the N–Cu–N coordination angles, the τ_4 parameters,[19] and the angles between coordination planes (Table 2).

Even if these parameters differ somehow along the series, there is no clear trend ascribable to the electronic characteristics of the *para*-substituents groups, suggesting that this effect is not the only determinant of the final structure of the dimers, and these differences are probably due to one global influence of these substituents (steric, electronic, and their ability to generate non covalent interactions) *i.e.*, they act in an unpredictable way over molecular structure as well as over dimer assembly and crystal packing.

The most important variation corresponds to the intraligand dihedral angle in the imine ligand. In this respect, inspection of Table 2 shows that those compounds with an extended stacking interaction present the smallest distortion, while compound [Cu(NN'-H)(PPh₃)Br] (the one with an unsubstituted phenyl-imine fragment and one single π–π interaction), shows the largest distortion with a dihedral angle >30°.

In order to find out if this possible relationship (*viz.*, the one between the extended stacking interaction and a reduction in the out-of-plane dihedral rotation in the imine ligand) was more general, we performed a systematic search in the CSD,[20] looking for transition metal complexes similar to those reported here. For this purpose, the compounds considered were restricted to have a four-coordinate transition metal bound to an NN′-R imine ligand with an eventual *para* R substituent, not longer than four (non-H) atoms in length. A total of 54 structures of that sort were found in the CSD, and the resulting histograms of the number of appearances as a function of the distortion angle are presented in Fig. 4, where the blue entries correspond to

Table 2 Selected coordination and noncovalent interaction parameters (distances/Å and angles/°) for [Cu(NN'-R)(PPh$_3$)Br] complexes

R	Spatial groups	τ_4	Orthogonal plane angles to metal centre	NCuN angle	NCCN torsion angle	Intraligand dihedral angle	Intra dimer···π-π··· stacking	Br···H3[a]	Br···Hi[a]	Br···H2[a]	Cu–Cu intra dimer	Br–Br intra dimer	Br···H4	Br···H5	Ph$_3$···Hp-Ph$_3$ π···T shape stacking
													Selected interdimer distances/Å		
							Selected distances for intra dimer units of complexes[a]/Å								
–NO$_2$	C2/c	0.8388	88.88 (PCuBr,N2CuN1) 76.60 (BrCuN1,N2CuP) 73.49 (BrCuN2,N1CuP)	79.07	−0.1(6)	4.63	3.738	3.127	3.020	3.550	6.69	7.438	2.896	3.431	3.380
–COCH$_3$	C2/c	0.8048	88.04 (PCuBr,N2CuN1) 74.34 (BrCuN1,N2CuP) 73.61 (BrCuN2,N1CuP)	79.09	2(1)	11.22	3.846	3.215	3.146	3.755	6.85	7.520	2.942	3.414	3.268
–H	P1̄	0.8219	86.15 (PCuBr,N2CuN1) 75.53(BrCuN1,N2CuP) 72.48 (BrCuN1,N2CuP)	79.01	−5.2(3)	30.15	3.647[b]		2.829[c]		8.04				
–CH$_3$	C2/c	0.8444	89.69 (PCuBr,N2CuN1) 73.49 (BrCuN1,N2CuP) 73.83 (BrCuN2,N1CuP)	79.08	1.9(5)	21.57	3.837	3.207	3.181	4.016	6.71	7.644	2.960	3.567	3.460
–OCH$_3$	P1̄	0.8282	83.93 (PCuBr,N2CuN1) 75.15 (BrCuN1,N2CuP) 70.13 (BrCuN2,N1CuP)	79.21	−2.9(5)	1.88	3.569	3.465	3.002	3.256	6.62	7.529	3.266	3.786	3.142
–N(CH$_3$)$_2$	P2$_1$/c	0.8599	86.18 (PCuBr,N2CuN1) 76.43 (BrCuN1,N2CuP) 73.57(BrCuN2,N1CuP)	79.65	3.5(3)	18.57	3.814	3.165	3.102	3.589	6.38	7.636	3.097	3.158	2.796

[a] Numbering of protons corresponds to that used for NMR assignment. [b] π–π stacking interaction. [c] π···T shape interaction, shown in the Fig. SI5b.
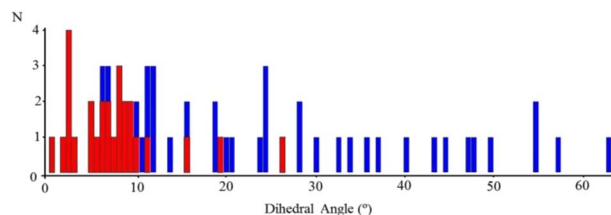
Fig. 4 Histograms of the number of appearances as a function of the distortion angle of the NN′-R imine ligand in similar transition metal complexes. Red entries correspond to complexes with centrosymmetric dimeric structures. Blue entries to complexes where no extended stacking is present. Obtained from the CSD.

complexes without extended stacking and the red ones to those with centrosymmetric dimeric structures.

These results strongly suggest a tendency to coplanarity of those NN′-R imine ligands that exhibit dimeric supramolecular interactions in the crystalline assembly, or, in other words, that due to the inter-molecular attractive force produced in the dimer, the imine ligand is forced to a more planar arrangement than expected for an ideal tetrahedral symmetry in single, not dimeric complexes.

Characterization of complexes and its self-assembly structures in solution by NMR spectroscopy

The ^{1}H-NMR spectra of all complexes exhibit only one set of narrow signals which shifted as a function of concentration as shown in Fig. 5 and SI6a to SI12a.† These results indicate the presence of chemical exchange in solution, thus, the observed ^{1}H NMR signals should be the consequence of the weighted average between more than one species in fast exchange on the NMR time scale at all the temperatures investigated (eqn (1)).

In a previous paper we described the same behaviour for [Cu(NN′-NO₂)(PPh₃)Br] complex and established the presence of a self-dimerization phenomenon in solution which involves
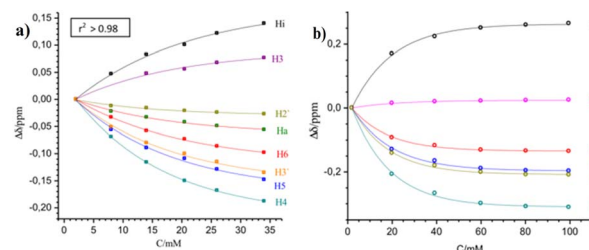
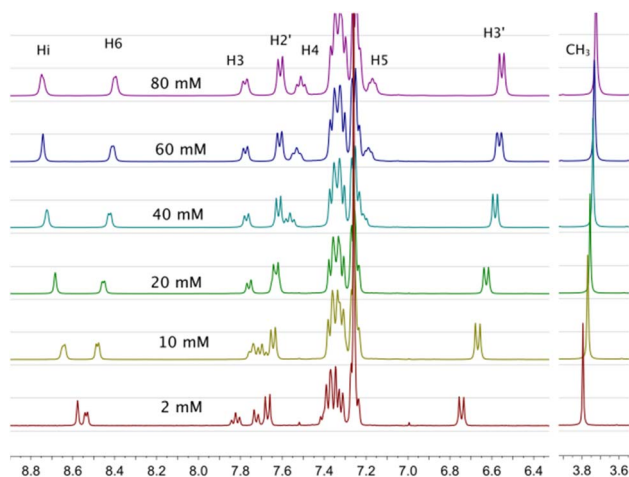**Fig. 6** Concentration effect on the chemical shifts of the NN'-R ligand protons for the [Cu(NN′-COCH₃)(PPh₃)Br] complex at 235 K (a) and for [Cu(NN′-Cl)(PPh₃)Br] at 220 K. (b) $\Delta\delta = \delta_i - \delta_0$, where δ_i correspond to δ observed at any concentration and δ_0 corresponds to the lowest concentration measured.

a fast equilibrium between a monomer complex and a supramolecular dimer supported by π–π stacking and C–H···Br interactions[12] (eqn (2)). An analysis similar to those used in the above paper allowed us to establish that the same behaviour is followed by the series of complexes whose study we are reporting now.

$$\delta_0 = \lambda_M\delta_M + \lambda_D\delta_D \qquad (1)$$

$$2\left[Cu(NN'\text{-}R)(PPh_3)Br\right] \ \overset{K_D}{\rightleftarrows}\ \left[Cu(NN'\text{-}R)(PPh_3)Br\right]_2 \quad (2)$$

The exponential dependence between the change in the resonance frequency of each proton ($\Delta\delta$) and the molar analytical concentration of the monomer is observed for most protons of this series of compounds (Fig. 6). Similar behaviour is seen for all the complexes at the different working temperatures studied, as shown in Fig. 6 for [Cu(NN′-COCH₃)(PPh₃)Br] and [Cu(NN′-Cl)(PPh₃)Br] (As similar in ESI, Fig. SI6b, SI7b, c, SI8b, c, SI10b, c, SI11b, c and SI12c†).

Dimerization was also confirmed by the presence of unexpected NOEs between protons which are distant from one another in the monomer structure. Indeed, NOESY crosspeaks can be observed between some protons of pyridine fragment (H3, H4, H5, H6) with the H2′ and H3′ protons of the 4-R-phenyl moiety of the NN′-R ligands (Fig. SI13†). These NOESY correlations are possible only when two ligands are assembled in an anti-conformation relative to an inversion centre placed between both complex units in a similar way to that in the crystal structures. This assembly of ligands resembles the one seen in the crystal packing and allows to establish that there is a great analogy between the assembly of the dimeric aggregates in the solid and those seen in the solution.

The exception is the [Cu(NN′-H)(PPh₃)Br] complex, which presents the same behaviour as the rest of the complexes in solution, but showing a different assembly in the crystal (*vide supra*). We can explain this behaviour considering that the noncovalent interactions through which these dimers pack in the solid are substituted by complex-solvent interactions in solution. These forces lead to self-dimerization of Cu(NN′-H)(PPh₃)Br] in the same structural shape as the other complexes.

Fig. 5 ^{1}H-NMR spectra of [Cu(NN′-OCH₃)(PPh₃)Br], $T = 220$ K, for several concentrations used to calculate self-association constants. Proton assignment is included. Similar behaviors were observed at different temperatures (see Tables SI3a to g†).
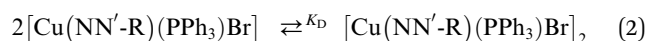
This dimerization assembling symmetry does not change the proton signals pattern of the NN'-R ligand in the dimer relative to the monomer but modifies the proton chemical environments changing their resonance frequencies. This is well established by the resonance dependence on both concentration and temperature in the ^{1}H-NMR spectra (Fig. 5, 6, and corresponding Fig. SI6 to SI12†).

As a result, increasing concentration produces progressive displacements of the resonance frequencies of the NN'-R ligand protons both, upfield as to downfield for the whole series of complexes at all the temperatures studied. In all the complexes, the H4, H5, H6, and H3′ protons of the NN'-R ligands show the more significant shift of proton frequencies to upfield ($-\Delta\delta$) as the complex's concentration increases (Fig. 6 and corresponding SI figures).†

This behaviour is the expected one for a self-association process through "face to face" π type stacking interaction between two nearby NN-R ligands, due to the fact that these protons are placed close to the shielding currents of the aromatic rings of another ligand in the supramolecular $[Cu(NN'-R)(PPh_3)Br]_2$ dimers.[21]

On the contrary, a progressive downfield shift ($+\Delta\delta$) occurs for Hi when the complex's concentration is increased. This deshielding effect is associated with the C–H⋯Br interaction,[22] considering that this proton is closer to the bromine ligand in the dimeric complexes, in the same way as in the crystalline structure (Fig. 3b, *vide supra*).

Thus, the resonance frequency of each proton is determined mainly by two non-covalent forces which cause an opposite effect in the observed chemical shifts in the process of self-dimerization, *i.e.*, AH⋯Br and π–π stacking. However, the relative contribution of these forces to the resonance frequency will be different for each proton depending on its position in the dimeric assembly.

However, H2′ and H3 protons move slightly towards lower or higher resonance frequencies, with temperature dependence (Tables SI3a to SI3g†) and not only toward the low fields as expected by their positions close to bromine in the crystalline packing. In those cases, we conclude that these protons undergo a compensatory influence of both π–π stacking and Br⋯H interactions and also suggest the presence of a large structural dynamism in the dimer.

The dimerization constants (K_D) of the self-dimerization equilibrium between a monomer and a dimeric supramolecular complex (eqn (2)) in CDCl$_3$ can be determined by the curve fitting method described by Horman and Dreux (eqn (3)),[23a] where the observed δ for a specific proton is a function of the analytical monomer concentration $[M]_0$.

$$\delta = \delta_M + (\delta_D - \delta_M)\left(\left(\frac{1}{4[M]_0 K_D}+1\right)\right.$$
$$\left.- \sqrt{\left(\frac{1}{4[M]_0 K_D}+1\right)^2 - 1}\right) \quad (3)$$

In this equation, δ_M and δ_D are the chemical shifts of the monomer and the dimer, respectively.

Using this self-dimerization model, we determine a set of K_D values, one for each of protons of the NN'-R ligands in each complex with good fitting values.[21,24]

We consider getting a representative K_D value for each complex averaging only the constants of the two protons that reach the highest $|\Delta\delta|$ in the measured concentration range (*i.e.* the greater $-\Delta\delta$ and $+\Delta\delta$ values at the highest concentrations) on the assumption that these protons should be influenced only by one of both assembly forces (AH⋯Br and stacking); but in fact, larger K_D values were obtained for protons that exhibit lower $|\Delta\delta|$ as the concentration increases (see Tables SI3a to SI3g†).

However, this is a commonly observed phenomenon in several compounds that experience self-association in solution.[9] As in those works, we decided to obtain a representative K_D values by averaging all calculated K_D's at each temperature, taking care that they were not very far from one another (Tables SI3a to g†). In addition, K_D values for protons that remain almost unperturbed by the opposite effect of noncovalent forces were not considered, for example, the H2′ and H3 protons.

We associate this behavior with the self-association equilibrium involving simultaneous rearrangements of the NN'-R ligand coplanarity (see X-ray) and the metal coordination environment (see electrochemical). Thus, both internal molecular rearrangements would be the cause of the variability found in

Table 3 Calculated dimerization constants, K_D, ΔH, ΔS and ΔG_{298K}/for [Cu(NN′-R)(PPh$_3$)Br] complexes in CDCl$_3$

	T/K								
–R	220	235	250	265	280	298	ΔH kcal^{-1} mol^{-1}	ΔS cal mol^{-1}	ΔG_{298} kcal^{-1} mol^{-1}
–NO$_2$[a]							−2.00	−0.67	−1.79
–COCH$_3$	21.4 ± 3.0	20.2 ± 3.1	19.0 ± 3.1	12.8 ± 3.0	11.7 ± 2.0	9.7 ± 3.7	−1.43	−0.19	−1.37
–H	9.0 ± 2.8	6.3 ± 1.4	6.4 ± 1.3	4.6 ± 0.5	4.0 ± 0.7	4.0 ± 0.8	−1.40	−2.09	−0.77
–CH$_3$	67.4 ± 22.7	47.5 ± 1.9	43.5 ± 7.0	36.6 ± 7.7	31.7 ± 12.1	29.3 ± 15.3	−1.35	2.08	−1.97
–OCH$_3$	35.2 ± 9.0	21.3 ± 3.5	20.1 ± 12.5	14.4 ± 4.9	9.3 ± 2.2	8.2 ± 2.9	−2.43	−4.02	−1.23
–N(CH$_3$)$_2$	24.3 ± 4.0	16.4 ± 2.3	12.4 ± 2.8	11.2 ± 4.3	9.3 ± 2.0	9.3 ± 1.9	−1.62	−1.25	−1.25
–Cl	69.4 ± 11.1	47.0 ± 3.5	31.3 ± 2.2	25.4 ± 4.7	18.6 ± 2.1	15.0 ± 2.4	−2.58	−3.35	−1.58

[a] Data from ref. 12.

the $\Delta\delta_H$ parameter and consequently, in the values of K_D for different protons in each complex.

The K_D average values for all complexes are given in Table 3, in the 210 to 298 K range and their values at all temperatures, are in the range 4 to 70 M^{-1}. These values are in the same range or just slightly higher than those seen for non-covalent organic dimers formed by π stacking depending on how extended of their aromatic systems.[21] Also, they have the same K_D values range reported for a few examples of self-dimerization in octahedral metal complexes where the intermolecular π–π stacking between the ligands is also dependent of fused ring extension.[9b,g] However, they are smaller than self-association constants exhibit by square planar complexes, but in these, their planarity and free apical positions allow a better intraligand π stacking and favour other types of non-covalent interactions such cation-ligand or metal–metal to yielder larger aggregate species.[9e,24,25]

As expected, these values decrease in each complex as temperature increases. Thus, from the dependence of the KD on temperature were determine the thermodynamic parameters ΔH and ΔS associated with the self-dimerization of [Cu(NN′-R)(PPh$_3$)Br] complexes from van't Hoff plots (Fig. 7 and Table 3). The linear fitting of all [Cu(NN′-R)(PPh$_3$)Br] complexes (R^2 values over 0.89) are in good agreement with the presence of a single thermodynamic process for the self-dimerization assembly in the studied temperature range (Fig. 7).

Although the $R^2 = 0.89$ in [Cu(NN′-COCH$_3$)(PPh$_3$)Br] can be considered a good linear fitting value for this system, two temperature regions with different slopes can also be assumed from the van't Hoff plot (Fig. 7). This behavior has been attributed to the thermodynamic phase change in the assembly geometry in supramolecular organic systems.[21b,27] However, we find that the values of the thermodynamic parameters determined from each slope are not very far from each other. Therefore, we conclude that the association symmetry of the

complex in the dimer remains unchanged in all temperature ranges, which is coherent with the frequency variation behaviour described previously ($-\Delta\delta$ and $+\Delta\delta$). We assume that the slightly low linear correlation is caused by the versatility of the non-covalent interactions to adapt the assembly shape to the different structural requirements of both monomer and dimer in a fast exchange.

The values of ΔH (range −1.4 to −2.6 kcal mol^{-1}), ΔS (range −0.2 to 2.1 cal mol^{-1} K^{-1}), and ΔG_{298} (range −0.8 to −2.0 kcal mol^{-1}) are of the same order for all complexes and are consistent with a spontaneous dimerization process enthalpically driven through the formation of both π–π and C–H⋯Br interactions (Table 3).

Electrochemical properties

Cyclic voltammetry (CV) and square wave voltammetry (SWV) experiments were performed pointing to the characterization of the effect of self-dimerization equilibrium observed by NMR (*vide supra*), on the electrochemical behavior of Cu(ɪ) complexes in dichloromethane solutions. Unlike NMR, the electrochemical study was carried out in CH$_2$Cl$_2$ instead of CH$_3$Cl because decomposition was observed in short periods of time under electrochemical conditions.

To validate the use of this solvent in electrochemical studies, the ^{1}H-NMR spectrum of the [Cu(NN′-OCH$_3$)(PPh$_3$)Br] complex in CD$_2$Cl$_2$ was performed to compare with those observed in CDCl$_3$ finding a high similarity between their spectral profiles (Fig. SI13h to i†). Subsequently, we evaluated the effect of ionic strength on the stability of the supramolecular self-association equilibrium, for which we carried out ^{1}H-NMR spectra measurements for both CDCl$_3$ and CD$_2$Cl$_2$ solution of the Cu(ɪ) complexes at concentrations similar to those used in electrochemical studies with increasing concentrations of supporting electrolyte (Fig. SI13j and k†). The results showed, (a) no spectral evidence of signals of species structurally different from those established in the NMR section (*vide supra*), (b) the presence of a chemical exchange process (c) that this chemical exchange follows a behavior similar to that observed without the electrolyte, (d) that the proton signals are shift as expected for an increasing of self-dimerization with an increase in ionic strength.

Both CV and SWV results show a similar electrochemical profile for all copper(ɪ) complexes between −0.7 to +0.4 V potential range *versus* Fc/Fc+ process like internal reference. These correspond to two not well-defined redox processes at anodic sweep and one process at cathodic sweep (Fig. 8 and Table 4). The redox processes are electrochemically irreversible ($\Delta E_p > 120$ mV and $I_{pa}/I_{pc} \neq 1$) and are diffusion controlled (see SI14 to SI17†).

As expected, in SWV experiments an increase of the intensities for both anodic peaks as the initial concentration of complexes increases are seen. However, when these curves are normalized by the absolute areas (total charge for both processes), it can be seen that the second peak increases its intensity while the first one decreases as concentration increases (Fig. 9 and SI19†).
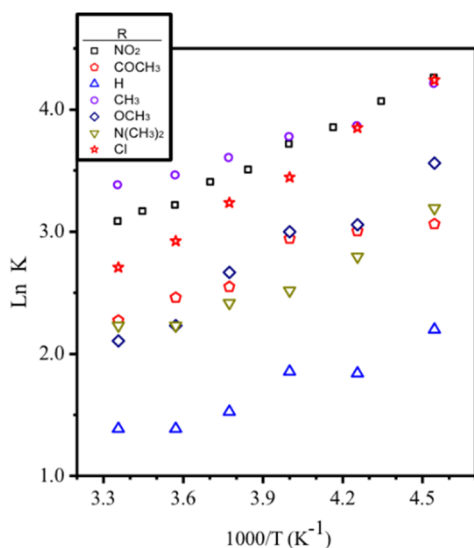

Fig. 7 van't Hoff plot for complexes in range of work temperature, 220 to 298 K.
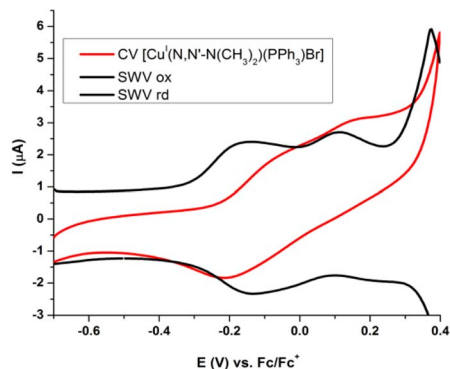
Fig. 8 Cyclic voltammetry and square wave voltammetry of [Cu(NN'-N(CH₃)₂)(PPh₃)Br] 1.0 mM, in CH₂Cl₂ and 0.1 M TBAP. SR = 50 mV s^{-1} at CV and 15 Hz to SWV.

Table 4 Electrochemical data for [Cu(NN'-R)(PPh₃)Br] complexes obtained by both cyclic voltammetry (CV) (scan rate 50 mV s^{-1}) and square wave voltammetry (SWV) (15 Hz in CH₂Cl₂) at 1.0 mM in CH₂Cl₂^a

	SWV. E/mV				CV. E/mV	
–R	E_{pa} M	E_{pa} D	E_{pc}	E_{pa} M	E_{pa} D	E_{pc}
–N(CH₃)₂	−137	110	−133	Sh	Sh	−215
–OCH₃	Sh	138	−181	Sh	182	−232
–CH₃	Sh	142	−101	Sh	196	−210
–H	Sh	130	−193	Sh	198	−245
–Cl	Sh	126	−113	Sh	172	−165
–COCH₃	Sh	186	−101	Sh	217	−164
–NO₂	Sh	170	−73	Sh	228	−129

^{a} Sh: shoulder, E_{pa} M: anodic peak potential of monomer, E_{pa} D: anodic peak potential of dimer, E_{pc}: cathodic peak potential.

In this way, the dependence of the ratio of two anodic peak-areas with the initial concentration of complex can be ascribed to the monomer–dimer equilibrium established by NMR studies (*vide supra*) in solution.

The electrochemical results show similar peak intensities for monomer and dimer, suggesting that their concentrations are of the same order of magnitude (Fig. 8). On the contrary, the association constants obtained by NMR in CDCl₃ without support electrolyte, indicate that the monomer concentration is more than one hundred times greater that of the dimer in solutions of same concentration as those used in electrochemical studies. This agrees with what was previously established through ¹H-NMR spectra where medium's ionic strength displaced the equilibrium to the dimer (Fig. SI13j and k†).[26]

Since equilibrium tends toward dimer formation when the concentration of the complexes is increased, the first anodic peak at the electrochemical process can be assigned to monomer and the higher anodic peak to the oxidation of the supramolecular dimer (Fig. 9 and SI19†).

Unexpectedly, both monomer and dimer have different redox features, which make possible their detection by electrochemical methods. These electrochemical differences between monomer and dimer may be interpreted in terms of
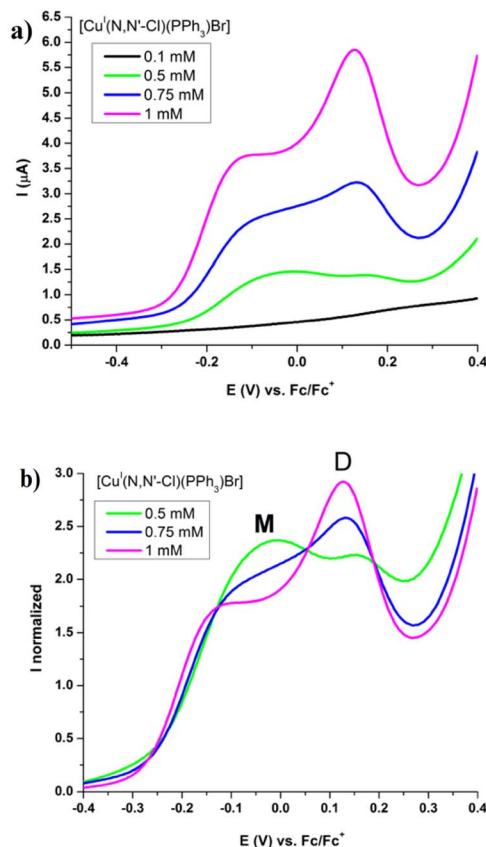

Fig. 9 (top a) SWV of [Cu(NN'-Cl)(PPh₃)Br] in CH₂Cl₂, 0.1 M TBAP, 15 Hz, at different initial concentrations. (down b) SWV normalized at absolute area for [Cu(NN'-Cl)(PPh₃)Br], at different initial concentrations. M = monomer; D = dimer.

the structural lability of the Cu(ɪ) center, allowing a structural rearrangement around this cation, due to the presence of previously discussed non-covalent interactions (π stacking and hydrogen bonding).

This structural lability has been associated with a d^{10} full electron configuration layer which does not provide crystal field stabilization of their complexes.[4,30a] Consequently, in the literature reports it is easily noted that the structures of Cu(ɪ) complexes are far from corresponding to tetrahedral symmetry, and may take practically all four-coordinate structures, pseudo-tetrahedral, trigonal pyramidal, see-saw, and pseudo-square-planar.[28]

Since the oxidation of Cu(ɪ) to Cu(ɪɪ) is associated with a geometric flattening of the molecule from pseudotetrahedral to square or square pyramidal, this process would occur with more positive oxidation potentials in complexes with a more tetrahedral coordination geometry assuming no other significant electronic effects. Indeed, in a previous work we observed in [Cu(biq)(Ph₂P-(CH₂)n)-PPh₂]ClO₄ (biq = 2,2-biquinoline) complexes the dependence of both Cu(ɪɪ)/Cu(ɪ) potential and the MLCT band with the Cu(ɪ) coordination geometry.[28a] We have also reported evidence of the ability of π-stacking intramolecular interactions to modulate a more tetrahedral geometry of a bimetallic helicate with respect to the corresponding bimetallic mesocate[4c] and the HOMO destabilization by the
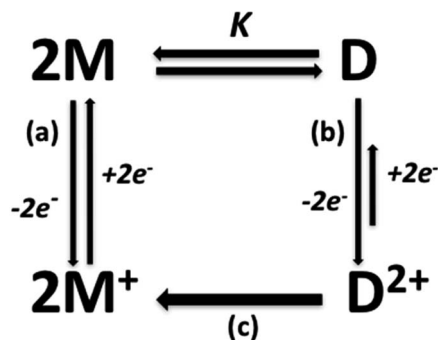
Fig. 10 Proposed mechanism for electrochemical process. (a) Electron transfer followed by conformational changes, (b) electron transfer, (c) conformational change and loss of supramolecular interactions.

effect of intermolecular noncovalent interactions in a supramolecular adduct {[Cu(biq)₂]-biq}.[9a]

So, considering that the anodic peaks of the dimer are located *ca.* 200 mV toward higher potential than those of the monomers in all complexes, it is possible to conclude that as self-assembly product, the ligands are forced towards a most orthogonal distribution among them in the dimer relative to the monomer.[29] The τ_4 crystal parameter for the complexes that are packed as supramolecular dimers, exhibit values over 0.8, indicating a metal centre structure closer to a tetrahedron.

The electrochemical irreversibility observed for the first oxidation process can be explained considering that this process is followed by a structural change, which is caused by the differences in the preferred coordination symmetry of copper ions, where Cu(I) complexes are closer to a tetrahedral symmetry, while Cu(II) prefers a more square-planar symmetry.[30]

Correspondingly, the dominant chemical irreversibility for the second Cu(II)/Cu(I) process can be explained considering that the anodic sweep could produce a Cu(II) dimer D_{2^+} which undergoes flattening and loss of supramolecular interactions (H⋯Br and π-stacking) due to the very rapid generation of Cu(II) monomers M^+, as shown in Fig. 10. In fact, a single dominant cathodic process instead, the cathodic peak associable to D_{2^+} reduction is very faint in all complexes (Fig. 8 and SI14 to SI17†).

Hammett parameter

Interested in rationalizing the electronic effects of peripheral *p*-substituents on the different properties of complexes, we plotted Hammett parameters for *R* (in NN'-R ligands)[31] *versus* several experimental parameters. For crystal data, Hammett parameters were plotted *vs.* τ_4, intraligand dihedral angle, intradimer π–π stacking distance, and NCCN torsion angle. In the same way, we plotted Hammett parameters *vs.* K_D constants at several temperatures and *vs.* ΔS and ΔH thermodynamic parameters obtained by NMR. Correlations were also investigated for the potential of Cu(II)/Cu(I) processes for dimer and monomer species. In all cases, poor correlation values (r^2) were obtained. Thus, the strength and geometry of

the assembly cannot be explained in terms of the electronic effect of the *p*-substituent. However, it can be rationalized by considering the cooperative contribution of both π–π stacking and Br⋯H interactions, while the electronic effect is usually determinant when only π–π interactions occur are predominant.

Experimental

Materials

All reactions were carried out under purified nitrogen (99.9%, Linde-Chile S.A.). The diethyl ether was dried and distilled according to standard procedures prior to use, and the other solvents were synthesis grade and used as received. The pyridine-2-carbaldehyde, 4-chloroaniline, 4-aminophenol, 4-nitroaniline, 4-anilineacetophenone, *N,N*-dimethyl-1,4-phenylenediamine (Merck) and 4-methoxyaniline, 4-methylaniline (Aldrich) were used as purchased. CuBr was prepared according to the reported procedure.[32] The [Cu{*N*-(4-nitrophenyl)pyridine-2-yl-methanimine} (PPh₃)Br] complex was previously reported.[12]

The specific synthetic procedures are reported in ESI.†

Instrumental

NMR spectrometer. ¹H, ¹³C{¹H} NMR, ³¹P{¹H} NMR, 2D-COSY, 2D-NOESY, ¹H¹³C 2D-HSQC-ed, and ¹H¹³C 2D-HMBC spectra, and the dimerization studies by proton NMR were performed on a Bruker Avance 400 MHz spectrometer (400.133 MHz for ¹H, 100.16 MHz for ¹³C, and 160.984 MHz for ³¹P) equipped with a 5 mm multinuclear broad-band dual probe head incorporating a *z*-gradient coil. All the measurements were made in CDCl₃. Chemical shifts were calibrated with respect to the solvent signal (7.26 ppm for proton residual solvent and 77.2 ppm for ¹³C) and referenced to TMS. ³¹P spectra were calibrated with respect to the external pattern H₃PO₄ 10%.

X-ray crystallography. X-ray diffraction experiments were performed at room temperature on an Oxford Diffraction Gemini CCD S Ultra diffractometer, with graphite monochromatized Mo Kα radiation ($\lambda = 0.7107$ Å). The structure was solved by direct methods (SHELXS97 and refined by least squares methods on F2 SHELXL-2014).[33,34]

Elemental analyses. Microanalysis was performed on a model EA-1108 Fisons elemental analyzer.

Electrochemical. All measurements were carried out under a nitrogen atmosphere at room temperature with tetrabutylammonium perchlorate (TBAP) 0.1 M as supporting electrolyte, Pt disc as working electrode (CH Instruments, USA), Pt wire as counter electrode, and Ag/AgCl(sat) as reference electrode, in a tree compartment cell using workstation Potentiostat 620D CH Instruments, USA. The cyclic voltammetry (CV) measurements were performed at different scan rates (10, 25, 50, 100, and 200 mV s⁻¹); square wave voltammetry (SWV) was carried out using a frequency of 15 Hz, increasing potential of 4 mV, amplitude potential of 25 mV. Cu(I) complexes were dissolved at different concentrations (1.00, 0.75, 0.50, 0.25, and 0.10 mM of monomer) in freshly distilled CH₂Cl₂. All potentials values were reported as *E vs.* internal reference F_c/F_{c^+}.

Preparation of complexes

The new series of [Cu(NN′-R)(PPh₃)Br] complexes were synthesized by the template condensation method from equimolar amounts of reagents.[2e,g,13]

To a dichloromethane/methanol (10/1) mixture solution of CuBr, dichloromethane/methanol solution of pyridine-2-carbaldehyde was added at room temperature, and after continuous stirring for 20 min, corresponding 4-substituted-aniline in the same solvents mixture was added and the solution mixture was stirred for 30 min. Subsequently, a solution of triphenylphosphine was added dropwise and stirred for 1 more hour at room temperature, forming a colored solution. The volume of solution was reduced in a rotary evaporator and the concentrate was precipitated with diethyl ether and washed with 2 × 5 mL of a diethyl ether/dichloromethane (9 : 1) mixture, and finally with 5 mL of diethyl ether.

The diffusion of diethyl ether vapour into a concentrated dichloromethane solution gave colored crystals ranging from orange to purple red which were adequate for crystallographic studies. Also, only crystallized materials were used for the spectroscopic and electrochemical studies.

General and specific synthetic procedure and NMR characterization data are reported in the experimental section and the ESI.†

Calculation of dimerization constants (K_D)

The values of K_D were determined by the method of Hormann and Dreux[23a] which relies on the gradual variation in the ¹H-NMR chemical shifts as a function of concentration at constant temperature. The procedure involves an iterative K_D, by fitting the observed chemical shift (δ_{obs}) of each proton using the mole fraction of dimer (eqn (3)) present at each concentration, starting from a reasonable guess of the association constant. The most accurate value of K_D is defined as that which yields the best linear relationship between δ_{obs} and the molar fraction (x_i)[21,24] (Tables SI3a to g†).

VT-NMR dimerization experiments

Solutions of complexes at different concentrations (in ranges of 2 to 100 mM according to each complex) were prepared in flasks of 1 and 2 mL with CDCl₃ (Aldrich). Proton NMR spectra for all solutions were recorded between 220 and 298 K at 15 K intervals. Each measurement was recorded after thermal equilibrium was established (*ca.* 3 min). The K_D values obtained at all temperatures were used to determine the thermodynamic parameter using the van't Hoff plot.

Hammett constants (σ) for substituents in the *p*-position of the *N*-phenyl ring of the imine ligands used in this work correspond to those published elsewhere.[31]

Conclusions

The whole series of mixed neutral Cu(ɪ) complexes studied crystallize in increasing organization, *i.e.* a tetrahedral distorted complex whose structure in a supramolecular dimer in turn packed in a crystal where the non-covalent interactions, π–π, and C–H⋯Br play the main role. The importance of these interactions is expressed in an enthalpy driven process of self-dimerization in solution between the monomer complex and discrete non-covalent dimers with a structure similar to that described in solid. The lack of correlation between Hammett constants of the *p*-substituents in *N*-phenyl fragments and several parameters obtained from NMR, X-ray, and electrochemical studies can be explained from the nature of the C–H⋯Br and π–π interactions. Since these interactions are more permissive of a spatial reordering of interacting fragments with respect to a covalent bond, they can remain linking the two complexes in a wide range of dimer conformations. Therefore, the noncovalent self-dimerization can involve the evolution of dimer from py/py assemblies toward one phenyl/py type in [Cu(NN′-H)(PPh₃)Br].

On the other hand, the significant Cu(ɪɪ)/Cu(ɪ) potential differences between both monomers and dimer complexes are consistent with the structurally labile character of Cu(ɪ), demonstrating that this ion can adapt its coordination geometry to structural requirements of supramolecular interactions. Thus, both the C–H⋯Br and π–π, interactions that assemble the complexes in the dimers, modify the coordination symmetry of Cu(ɪ) towards more tetrahedral geometry stabilizing the HOMO of the dimer with respect to the monomer.

Consequently, here we provide an experimental background of the remarkable influence of supramolecular interactions on the structure and properties of Cu(ɪ) complexes through their ability to modulate the metal coordination symmetry and the coordinative stability to avoid dissociative equilibria. In addition, these results allow us to hypothesize that through supramolecular structuring it is possible to simultaneously obtain both effects, decrease the conformational mobility and increase the chemical stability of Cu(ɪ) complexes as an alternative to intramolecular architectural molecular designs, which is the most researched strategy.

Author contributions

Conceptualization: JG, CV, RB. Investigation, experimental design, and formal analysis: JG, CV, RB, EF, JC-V, DHJ. Experimental data collection: DHJ, JC-V, FM, CV, CPS, EF, RB. Validation: JG, CV, RB, JC, LL. Funding acquisition: JG, CV. Writing (original draft): JG, CV, RB. Writing (review & editing): JG, CV, RB, JC, LL.

Conflicts of interest

There are no conflicts to declare.

Acknowledgements

Notes and references

1 (a) B. Bozic-Weber, E. C. Constable, C. E. Housecroft, M. Neuburger and J. R. Price, *Dalton Trans.*, 2010, **39**, 3585; (b) C. Cunningham, J. Moore, K. Cunningham, P. Fanwick and D. McMillin, *Inorg. Chem.*, 2000, **39**, 3638; (c) M. Miller, P. Gantzel and T. Karpishin, *Inorg. Chem.*, 1998, **37**, 2285; (d) M. Meyer, A. Albrecht-Gary, C. Dietrich-Buchecker and J. Sauvage, *Inorg. Chem.*, 1999, **38**, 2279; (e) M. Eggleston, P. Fanwick, A. Pallenberg and D. McMillin, *Inorg. Chem.*, 1997, **36**, 4007; (f) A. Pallenberg, K. Koenig and D. Barnhart, *Inorg. Chem.*, 1995, **34**, 2833; (g) N. Navon, G. Golub, H. Cohen, P. Paoletti, B. Valtancoli, A. Bencini and D. Meyerstein, *Inorg. Chem.*, 1999, **38**, 3484; (h) D. Scaltrito, D. Thompson, J. O'Callaghan and G. Meyer, *Coord. Chem. Rev.*, 2000, **208**, 243; (i) D. Schultz, F. Biaso, A. Shahi, M. Geoffroy, K. Rissanen, L. Gagliardi, C. Cramer and J. R. Nitschke, *Chem.–Eur. J.*, 2008, **14**, 7180; (j) M. Miller and T. Karpishin, *Inorg. Chem.*, 1999, **38**, 5246; (k) N. Armaroli, G. Accorsi, F. Cardinali and A. Listorti, *Top. Curr. Chem.*, 2007, **280**, 69; (l) Y. Liu, S. Yiu, C. Ho and W. Wong, *Coord. Chem. Rev.*, 2018, **375**, 514; (m) S. Brauchli, F. Malzner, E. Constable and C. Housecroft, *RSC Adv.*, 2014, **4**, 62728; (n) M. Nishikawa, S. Kume and H. Nishihara, *Phys. Chem. Chem. Phys.*, 2013, **15**, 10549; (o) M. Nishikawa, Y. Takara, Y. Hattori, K. N omoto, T. Kusamoto, S. Kume and H. Nishihara, *Inorg. Chem.*, 2013, **52**, 8962; (p) S. Sawant, G. Gaikwad, V. Sawant, B. Yamgar and S. Chavan, *Inorg. Chem. Commun.*, 2009, **12**, 632; (q) G. Ardizzoia, S. Brenna, F. Castelli and S. Galli, *Inorganica Chim. Acta*, 2009, **362**, 3507; (r) L. Ravaro, K. Zanoni and A. de Camargo, *Energy Rep.*, 2020, **6**, 37; (s) C. Smith, C. Branham, B. Marquardt and K. Mann, *J. Am. Chem. Soc.*, 2010, **132**(40), 14079.

2 (a) S. Saha, P. Biswas and M. Schmittel, *Inorg. Chem.*, 2019, **58**, 3466; (b) J. M. Lehn, A. Rigault, J. Siegel, J. Harrowfield, B. Chevrier and D. Moras, *Proc. Natl. Acad. Sci.*, 1987, **84**, 2565; (c) A. Goswami, S. Saha, P. Biswas and M. Schmittel, *Chem. Rev.*, 2019, **120**, 125; (d) S. Neogi, Y. Lorenz, M. Engeser, D. Samanta and M. Schmittel, *Inorg. Chem.*, 2013, **52**, 6975; (e) J. Fan, J. Bats and M. Schmittel, *Inorg. Chem.*, 2009, **48**, 6338; (f) S. Neogi, G. Schnakenburg, Y. Lorenz, M. Engeser and M. Schmittel, *Inorg. Chem.*, 2012, **51**, 10832; (g) M. Schmittel and J. Fan, *Org. Lett.*, 2011, **13**, 3916; (h) R. Forgan, J. Sauvage and J. Stoddart, *Chem. Rev.*, 2011, **111**, 5434; (i) C. Piguet, M. Borkovec, J. Hamacek and K. Zeckert, *Coord. Chem. Rev.*, 2005, **249**, 705; (j) M. Maekawa, T. Hayashi, K. Sugimoto, T. Okubo and T. Kuroda-Sowa, *Inorganica Chim. Acta*, 2019, **497**, 119088; (k) B. Schoentjes and J. M. Lehn, *Helv. Chim. Acta*, 1995, **78**, 1; (l) M. Schmittel, V. Kalsani and J. Bats, *Inorg. Chem.*, 2005, **44**, 4115.

3 (a) Y. Liu, Y. Ma, J. Yang, C. Diercks, N. Tamura, F. Jin and O. Yaghi, *J. Am. Chem. Soc.*, 2018, **140**, 16015; (b) M. Saha, S. Pramanik and M. Schmittel, *Chem. Commun.*, 2012, **48**, 9459; (c) Y. Liu, Y. Ma, Y. Zhao, X. Sun, F. Gándara, H. Furukawa, Z. Liu, H. Zhu, C. Zhu, K. Suenaga, P. Oleynikov, A. Alshammari, X. Zhang, O. Terasaki and O. Yaghi, *Science*, 2016, **351**, 365; (d) C. Kepert, P. Southon, S. Brooker and R. Miller, *Inorg. Chem.*, 2016, **55**, 6195; (e) Q. L. Ni, X. F. Jiang, L. C. Gui, X. J. Wang, K. G. Yang and X. S. Bi, *New J. Chem.*, 2011, **35**, 2471; (f) Y. Liu, C. Diercks, Y. Ma, H. Lyu, C. Zhu, S. Alshmimri, S. Alshihri and O. Yaghi, *J. Am. Chem. Soc.*, 2019, **141**, 677.

4 (a) E. Leoni, J. Mohanraj, M. Holler, M. Mohankumar, I. Nierengarten, F. Monti, A. Sournia-Saquet, B. Delavaux-Nicot, J. Nierengarten and N. Armaroli, *Inorg. Chem.*, 2018, **57**, 15537; (b) E. Riesgo, Y. Hu, F. Bouvier and R. Thummel, *Inorg. Chem.*, 2001, **40**, 2541; (c) D. Díaz, L. Llanos, P. Arce, R. Lorca, J. Guerrero, J. Costamagna, D. Aravena, G. Ferraudi, A. Oliver, G. Lappin and L. Lemus, *Chem.–Eur. J.*, 2018, **24**, 13839; (d) A. Kaeser, M. Mohankumar, J. Mohanraj, F. Monti, M. Holler, J. Cid, O. Moudam, I. Nierengarten, L. Karmazin-Brelot, C. Duhayon, B. Delavaux-Nicot, N. Armaroli and J. Nierengarten, *Inorg. Chem.*, 2013, **52**, 12140.

5 (a) M. Miller, P. Gantzel and T. Karpishin, *Angew. Chem., Int. Ed.*, 1998, **37**, 1556; (b) D. Datta and A. Chakravorty, *Inorg. Chem.*, 1983, **22**, 1085; (c) L. Lemus, J. Guerrero, J. Costamagna, G. Estiu, G. Ferraudi, A. Lappin, A. Oliver and B. Noll, *Inorg. Chem.*, 2010, **49**, 4023; (d) L. Lemus, J. Guerrero, J. Costamagna, R. Lorca, D. H. Jara, G. Ferraudi, A. Oliver and A. G. Lappin, *Dalton Trans.*, 2013, **42**, 11426.

6 (a) M. Miller, P. Gantzel and T. Karpishin, *J. Am. Chem. Soc.*, 1999, **121**, 4292; (b) C. Cunningham, K. Cunningham, J. Michalec and D. McMillin, *Inorg. Chem.*, 1999, **38**, 4388; (c) M. Eggleston, D. McMillin, K. Koenig and A. Pallenberg, *Inorg. Chem.*, 1997, **36**, 172; (d) M. Ruthkosky, F. Castellano and G. Meyer, *Inorg. Chem.*, 1996, **35**, 6406; (e) D. McMillin, J. Kirchhoff and K. Goodwin, *Coord. Chem. Rev.*, 1985, **64**, 83; (f) L. Llanos, C. Vera, A. Vega, D. Aravena and L. Lemus, *Inorg. Chem.*, 2020, **59**, 15061.

7 (a) P. Oguadinma, A. Rodrigue-Witchel, C. Reber and F. Schaper, *Dalton Trans.*, 2010, **39**, 8759; (b) T. Nicholls, C. Caporale, M. Massi, M. Gardiner and A. Bissember, *Dalton Trans.*, 2019, **48**, 7290; (c) J. Fan, Y. Zhang, K. Zhang, J. Liu, G. Jiang, L. Lin and C. Wang, *Org. Electron.*, 2019, **71**, 113; (d) G. Filonenko, R. Fayzullin and J. Khusnutdinova, *J. Mater. Chem. C*, 2017, **5**, 1638; (e) P. Papanikolaou, J. Mohanraj, A. Czapik, M. Gdaniec, G. Accorsi and P. Akrivos, *Dalton Trans.*, 2013, **42**, 3357; (f) M. Fraser, H. van der Salm, S. Cameron, J. Barnsley and K. Gordon, *Polyhedron*, 2013, **52**, 623; (g) L. Kohler, R. Hadt, D. Hayes, L. Chen and K. Mulfort, *Dalton Trans.*, 2017, **46**, 13088; (h) M. Fraser, H. van der Salm, S. Cameron, A. Blackman and K. Gordon, *Inorg. Chem.*, 2013, **52**, 2980.

8 (a) S. Kammer, A. Kelling, H. Baier, W. Mickler, C. Dosche, K. Rurack, A. Kapp, F. Lisdat and H. Holdt, *Eur. J. Inorg. Chem.*, 2009, **31**, 4648; (b) S. Kammer, I. Starke, A. Pietrucha, A. Kelling, W. Mickler, U. Schilde, C. Dosche, E. Kleinpeter and H. Holdt, *Dalton Trans.*, 2012, **41**, 10219;

(c) M. Stollenz, H. Gehring, V. Konstanzer, S. Fischer, S. Dechert, C. Grosse and F. Meyer, *Organometallics*, 2011, **30**, 3708; (d) Y. Jahng, J. Hazelrigg, D. Kimball, E. Riesgo and F. Wu andR. P. Thummel, *Inorg. Chem.*, 1997, **36**, 5390; (e) L. Zhang, B. Li and Z. Su, *Langmuir*, 2009, **25**, 2068; (f) S. Kuang, D. Cuttell, D. McMillin, P. Fanwick and R. Walton, *Inorg. Chem.*, 2002, **41**, 3313.

9 (a) N. Martínez, M. Isaacs, A. Oliver, G. Ferraudi, G. Lappin and J. Guerrero, *Dalton Trans.*, 2018, **47**, 13171; (b) D. Gut, A. Rudi, J. Kopilov, I. Goldberg and M. Kol, *J. Am. Chem. Soc.*, 2002, **124**, 5449; (c) N. De Tacconi, R. Chitakunye, F. MacDonnell and R. Lezna, *J. Phys. Chem. A*, 2008, **112**, 497; (d) R. Liu, M. Huang, X. Yao, H. Li, F. Yang and X. Li, *Inorganica Chim. Acta*, 2015, **434**, 172; (e) I. Kotzé, W. Gerber, J. Mckenzie and K. Koch, *Eur. J. Inorg. Chem.*, 2009, **12**, 1626; (f) S. Bergman, D. Reshef, S. Groysman, I. Goldberga and M. Kol, *Chem. Commun.*, 2002, 2374; (g) S. Bergman, D. Reshef, L. Frish, Y. Cohen, I. Goldberg and M. Kol, *Inorg. Chem.*, 2004, **43**, 3792.

10 (a) S. Chavan, S. Sawant, S. Pawal and M. More, *Polyhedron*, 2016, **105**, 192; (b) S. Chavan, S. Sawant, V. Sawant and G. Lahiri, *Inorg. Chem. Commun.*, 2011, **14**, 1373; (c) S. Chavan, S. Sawant, V. Sawant and G. Lahiri, *Inorganica Chim. Acta*, 2010, **363**, 3359; (d) D. Seth and S. Bhattacharya, *Polyhedron*, 2011, **30**, 2438; (e) D. Tzimopoulos, S. Brenna, A. Czapik, M. Gdaniec, A. Ardizzoia and P. Akrivos, *Inorganica Chim. Acta*, 2012, **383**, 105; (f) H. Zhao, B. Huang, Y. Wu and M. Cai, *J. Organomet. Chem.*, 2015, **797**, 21.

11 (a) S. Shakhatreh, J. Mohanraj, A. Czapik, D. Tzimopoulos, S. Kotoulas, M. Gdaniec and P. Akrivos, *J. Mol. Struct.*, 2011, **1002**, 51; (b) T. Huang, J. Yan, H. Yang, H. Dum and M. Zhang, *J. Coord. Chem.*, 2015, **68**, 1514; (c) T. Huang and M. Zhang, *Aust. J. Chem.*, 2014, **67**, 887.

12 D. Jara, L. Lemus, L. Farías, E. Freire, R. Baggio and J. Guerrero, *Eur. J. Inorg. Chem.*, 2012, **10**, 1579.

13 (a) T. Ronson, S. Zarra, S. Black and J. Nitschke, *ChemComm*, 2013, **49**, 2476; (b) M. Smulders, A. Jiménez and J. Nitschke, *Angew. Chem., Int. Ed.*, 2012, **51**, 6681; (c) K. Hänni and D. Leigh, *Chem. Soc. Rev.*, 2010, **39**, 1240.

14 (a) S. Dehghanpour, A. H. Mahmoudkhani and M. Amirnasr, *Struct. Chem.*, 2006, **17**, 255; (b) G. Saha, K. Sarkar, T. Mondal and C. Sinha, *Inorganica Chim. Acta*, 2012, **387**, 240; (c) A. Khalaji, S. Peyghoun, A. Akbari, N. Feizi, M. Dusek and V. Eigner, *Polyhedron*, 2016, **19**, 429; (d) G. Saha, C. Patra, P. Datta, K. Sarkar, R. Saha, C. Chen and C. Sinha, *Polyhedron*, 2015, **87**, 63.

15 (a) A. Hasheminasab, L. Wang, M. Dawadi, J. Bass, R. Herrick, J. Rack and C. Ziegler, *Dalton Trans.*, 2015, **44**, 15400; (b) A. Hasheminasab, J. Engle, J. Bass, R. Herrick and C. Ziegler, *Eur. J. Inorg. Chem.*, 2014, **16**, 2643; (c) R. Dominey, B. Hauser, J. Hubbard and J. Dunham, *Inorg. Chem.*, 1991, **30**, 4754.

16 (a) L. Gonsalvi, J. Gaunt, H. Adams, A. Castro, G. Sunley and A. Haynes, *Organometallics*, 2003, **22**, 1047; (b) D. Kanas, S. Geier, C. Vogels, A. Decken and S. Westcott, *Inorg.*

Chem., 2008, **47**, 8727; (c) S. Mak, V. Yam, C. Che and T. Mak, *J. Chem. Soc., Dalton Trans.*, 1990, **8**, 2555.

17 (a) R. Dhiman and C. Nagaraja, *New J. Chem.*, 2019, **43**, 13662; (b) J. Schöffel, N. Šušnjar, S. Nückel, D. Sieh and P. Burger, *Eur. J. Inorg. Chem.*, 2010, **31**, 4911; (c) G. Li, Y. Wu, G. Shan, W. Che, D. Zhu, B. Song, L. Yan, Z. Sua and M. Bryce, *Chem. Commun.*, 2014, **50**, 6977.

18 (a) M. Nishio, *CrystEngComm*, 2004, **6**, 130; (b) C. Janiak, *J. Chem. Soc., Dalton Trans.*, 2000, **21**, 3885; (c) C. Hunter, K. Lawson, J. Perkins and C. Urch, *J. Chem. Soc., Perkin Trans. 1*, 2001, **5**, 651; (d) C. Hunter and J. Sanders, *J. Am. Chem. Soc.*, 1990, **112**, 5525; (e) M. Nishio, Y. Umezawa, K. Honda, S. Tsuboyama and H. Suezawa, *CrystEngComm*, 2009, **11**, 1757; (f) Z. Zhang, Y. Luo, J. Chen, S. Dong, Y. Yu, Z. Ma and F. Huang, *Angew. Chem., Int. Ed.*, 2011, **50**, 1397; (g) Y. Umezawa, S. Tsuboyama, K. Honda, J. Uzawa and M. Nishio, *Bull. Chem. Soc. Jpn.*, 1998, **71**, 1207; (h) M. Nishio, Y. Umezawa, J. Fantini, M. Weiss and P. Chakrabarti, *Phys. Chem. Chem. Phys.*, 2014, **16**, 12648; (i) H. Brunner, *Acta Crystallogr., Sect. B: Struct. Sci.*, 2002, **58**, 380.

19 L. Yang, D. Powell and R. Houser, *Dalton Trans.*, 2007, **9**, 955.

20 F. Allen, *Acta Crystallogr., Sect. B: Struct. Sci.*, 2002, **58**, 380.

21 (a) C. Xiao, M. Wu, Y. Zhang, X. Zhao, J. Yu and X. Zheng, *Magn. Reson. Chem.*, 2014, **52**, 460; (b) H. Sun, K. Ye, C. Wang, H. Qi, F. Li and Y. Wang, *J. Phys. Chem. A*, 2006, **110**, 10750; (c) N. Marchettini, G. Valensin and E. Gaggelli, *Biophys. Chem.*, 1990, **36**, 65; (d) A. Thakkar, L. Tensmeyer and W. Wilham, *J. Pharm. Sci.*, 1971, **60**, 1267.

22 (a) J. Del Bene, S. Perera and R. Bartlett, *J. Phys. Chem. A*, 1999, **103**, 8121; (b) K. Mizuno, T. Ochi and Y. Shindo, *J. Chem. Phys.*, 1998, **109**, 9502; (c) R. Kaur, M. Ramesh, P. Bharatam and R. Kishore, *J. Phys. Chem. B*, 2014, **118**, 9199; (d) J. Purcell, H. Susi and J. Cavanaugh, *Can. J. Chem.*, 1969, **47**, 3655; (e) M. Natalia, C. Zarycz and C. Fonseca, *J. Phys. Chem. Lett.*, 2018, **9**, 3720.

23 (a) I. Horman and B. Dreux, *Helv. Chim. Acta*, 1984, **67**, 754; (b) R. Martin, *Chem. Rev.*, 1996, **96**, 3043.

24 K. Koch, C. Sacht and C. Lawrence, *J. Chem. Soc., Dalton Trans.*, 1998, **4**, 689.

25 (a) I. Kotzé, W. Gerber, Y. Wu and K. Koch, *Dalton Trans.*, 2013, **42**, 3791; (b) V. Sivchik, E. Grachova, A. Melnikov, S. Smirnov, A. Ivanov, P. Hirva, S. Tunik and I. Koshevoy, *Inorg. Chem.*, 2016, **55**, 3351.

26 (a) V. Steullet and D. Dixon, *J. Chem. Soc., Perkin Trans. 2*, 1999, 1547; (b) H. Hwang, S. Lee, S. Lee and J. Park, *J. Chem. Soc., Perkin Trans. 2*, 1999, 1081.

27 H. Sun, Y. Zhao, Z. Huang, Y. Wang and F. Li, *J. Phys. Chem. A*, 2008, **112**, 11382.

28 (a) J. Guerrero, L. Cortez, L. Lemus, L. Farías, J. Costamagna, C. Pettinari, M. Rossi and F. Caruso, *Inorganica Chim. Acta*, 2010 **363**, 380; (b) M. Lazorski and F. Castellano, *Polyhedron*, 2014, **82**, 57; (c) M. Magni, A. Colombo, C. Dragonetti and P. Mussini, *Electrochim. Acta*, 2014, **141**, 324; (d) K. Kubicek, S. Veedu, D. Storozhuk, R. Kia and S. Techert, *Polyhedron*, 2017, **124**, 166.

29 (a) T. Lan and W. Wang, *Sens. Actuators, B*, 2018, **254**, 81; (b) Y. Wang, S. Li, L. Wang, S. Qu and K. Liu, *J. Lumin.*, 2017, **192**, 269; (c) Y. Zhao, Y. Van, D. Wang, L. Li and P. Qiu, *J. Mol. Struct.*, 2019, **1181**, 171.

30 (a) Y. Zhang, M. Schulz, M. Wächtler, M. Karnahl and B. Dietzek, *Coord. Chem. Rev.*, 2018, **356**, 127; (b) M. Mara, N. Jackson, J. Huang, A. Stickrath, X. Zhang, N. Gothard, M. Ratner and L. Chen, *J. Phys. Chem. B*, 2013, **117**, 1921; (c) S. Garakyaraghi, E. Danilov, C. McCusker and F. Castellano, *J. Phys. Chem. A*, 2015, **119**, 3181.

31 (a) B. Jovanović, M. Mišić-Vuković, A. Marinković and V. Vajs, *J. Mol. Struct.*, 2002, **642**, 113; (b) D. McDaniel and H. Brown, *J. Org. Chem.*, 1958, **23**, 420; (c) C. Hansch, A. Leo and R. Taft, *Chem. Rev.*, 1991, **91**, 165; (d) R. Akaba, H. Sakuragi and K. Tokumaru, *Bull. Chem. Soc. Jpn.*, 1985, **58**, 1711.

32 (a) S. Bertz, E. Fairchild, I. Denissova and L. Barriault, *Encyclopedia of Reagents for Organic Synthesis*, 2001; (b) R. Keller, H. Wrcoff and L. Marchi, *Inorg. Synth.*, 1946, **2**, 1.

33 G. M. Sheldrick, SHELXS97, *Acta Crystallogr., Sect. A: Found. Crystallogr.*, 2008, **64**, 112.

34 G. M. Sheldrick, SHELXL-2014, *Acta Crystallogr., Sect. C: Cryst. Struct. Commun.*, 2015, **71**, 8.